LOCAL PERCEPTION AND LEARNING MECHANISMS IN RESOURCE-CONSUMER DYNAMICS*

QINGYAN SHI[†], YONGLI SONG[‡], AND HAO WANG[§]

Abstract. Spatial memory is key in animal movement modeling, but it has been challenging to explicitly model learning to describe memory acquisition. In this paper, we study novel cognitive consumer-resource models with different consumer's learning mechanisms and investigate their dynamics. These models consist of two PDEs in composition with one ODE such that the spectrum of the corresponding linearized operator at a constant steady state is unclear. We describe the spectra of the linearized operators and analyze the eigenvalue problem to determine the stability of the constant steady state. We then perform bifurcation analysis by taking the memory-based diffusion rate as the bifurcation parameter. It is found that steady-state and Hopf bifurcations can both occur in these systems, and the bifurcation points are given so that the stability region can be determined. Moreover, rich spatial and spatiotemporal patterns can be generated in such systems via different types of bifurcation. Our effort establishes a new approach to tackle a hybrid model of PDE-ODE composition and provides a deeper understanding of cognitive movement-driven consumer-resource dynamics.

Key words. memory-based diffusion, resource-consumer, PDE-ODE model, pattern formation, Hopf bifurcation, steady-state bifurcation

AMS subject classifications. 34K18, 92B05, 35B32, 35K57

1. Introduction.

Since 1952, Turing instability Turing induced by random diffusion has been highly esteemed as the mechanism for the spatial heterogeneous distribution of species in nature. However, numerous pieces of evidence show that random diffusion is insufficient to describe the animal movement as many factors may affect the animals' decision for spatial movement. Some clever animals even have an amazing ability to choose their favored habitat. Therefore, animal cognition should be taken into account in animal movement modeling [6, 8, 18]. Although specific mechanisms are still in debate, most modelers believe that perception (information acquisition) and memory (the retention of information) play dominant roles in interpreting complicated animal movement behaviors. Generally speaking, perception is the process by which animals acquire information, while memory is the storage, encoding, and recalling of information. Spatial memory is the memory of spatial locations in a living organism's landscape. A strong motivation for the importance of spatial memory in animal movements is the empirical evidence of blue whale migrations presented by [1] and discussed by [4]. Much progress has been made in incorporating spatial cognition or memory implicitly, such as home range analysis [16, 17], scent marks [11],

*Submitted to the editors DATE.

Funding: The first author is partially supported by the National Natural Science Foundation of China (No.12001240,12271216) and the Natural Science Foundation of Jiangsu Province (No.BK20200589). The second author is supported by the National Natural Science Foundation of China (No.12371166) and the Zhejiang Provincial Natural Science Foundation of China (No.LZ23A010001). The third author is partially supported by the Natural Sciences and Engineering Research Council of Canada (Individual Discovery Grant RGPIN-2020-03911 and Discovery Accelerator Supplement Award RGPAS-2020-00090) and the Canada Research Chairs program (Tier 1 Canada Research Chair Award).

[†]School of Science, Jiangnan University, Wuxi, Jiangsu, 214122, China. (qingyanshi@jiangnan.edu.cn).

[‡]School of Mathematics, Hangzhou Normal University, Hangzhou, Zhejiang, 311121, China. (songyl@hznu.edu.cn).

[§]Corresponding Author. Department of Mathematical and Statistical Sciences, University of Alberta, Edmonton, AB T6G 2G1, Canada. (hao8@ualberta.ca).

taxis-driven pattern formation [20, 21], information gaining through the last visit to locations [22], perceptual ranges [5], and delayed resource-driven movement [7].

In [5], Fagan et al. proposed a resource-driven movement model to study perceptual ranges and foraging success, and the delay effect was later considered in the resource-driven movement model in [7]. In [35], by assuming that the consumers have knowledge of where the resources are, Wang and Salmaniw proposed the following consumer-resource model with an additional term biasing the movement of the consumer:

$$
(1.1)\qquad \begin{cases} u_t = d_1\Delta u + u\left(1-\dfrac{u}{k}\right) - \dfrac{muv}{1+u}, & x\in\Omega,\ t>0,\\ v_t = d_2\Delta v - \chi\nabla\cdot(v\nabla\bar{q}) + \dfrac{muv}{1+u} - dv, & x\in\Omega,\ t>0,\\ \partial_n u = \partial_n v = 0, & x\in\partial\Omega,\ t>0, \end{cases}
$$

where $u = u(x,t)$ and $v = v(x,t)$ denote the density of resource and consumer, respectively. The attractive potential $\bar{q}(x,t)$ is of the form

$$
\bar{q}(x,t) = \int_\Omega g(x-y)q(y,t)dy,
$$

where $g(x-y)$ is the perceptual kernel and for the biological meaning, $g(x)$ should satisfy the following hypotheses [35]:

(i) $g(x)$ is symmetric about the origin and non-increasing from the origin;

(ii) $\int_\Omega g(x)dx = 1$, and $\lim\limits_{R\to 0^+} g(x) = \delta(x)$.

The typical example that satisfies the above two hypotheses is the so-called top-hat function:

$$
g(x-y) = \begin{cases} \dfrac{1}{2R}, & -R < x-y < R,\\ 0, & \text{otherwise,} \end{cases}
$$

where R is the perceptual range. Recently, there has been an increasing interest and effort in studying the influence of perceptual range on population dynamics [?, 35, 39].

In this paper, we explore the limiting scenario when the perceptual range approaches zero, i.e., $R \to 0^+$. For this local perception scenario, $g(x) = \delta(x)$ and system (1.1) becomes

$$
(1.2)\qquad \begin{cases} u_t = d_1\Delta u + u\left(1-\dfrac{u}{k}\right) - \dfrac{muv}{1+u}, & x\in\Omega,\ t>0,\\ v_t = d_2\Delta v - \chi\nabla\cdot(v\nabla q) + \dfrac{muv}{1+u} - dv, & x\in\Omega,\ t>0,\\ \partial_n u = \partial_n v = 0, & x\in\partial\Omega,\ t>0. \end{cases}
$$

The parameters in (1.2) are all positive constants except for $\chi\in\mathbb{R}$: $d_1,\ d_2$ denote the random diffusion rates for resource and consumer, respectively; k is the carrying capacity for resource; m is the predation rate; $\chi > 0 (< 0)$ implies that the consumer follows an attractive (repulsive) movement to the high-density area based on the perception of the population density.

In [35], Wang and Salmaniw proposed that $q(x,t)$ is a cognitive map based on the learning and memory waning of the consumer and satisfies either of the following two ODEs:

$$
(1.3)\qquad \begin{aligned} &\mathrm{H1}: q_t = bu - \gamma q,\\ &\mathrm{H2}: q_t = buv - (\gamma + \xi v)q. \end{aligned}
$$

When the cognitive map $q(x,t)$ satisfies (H1), then Eq.(1.2) becomes

$$
\begin{cases}
u_t = d_1\Delta u + u\left(1-\dfrac{u}{k}\right) - \dfrac{muv}{1+u}, & x\in\Omega,\ t>0,\\
v_t = d_2\Delta v - \chi\nabla\cdot(v\nabla q) + \dfrac{muv}{1+u} - dv, & x\in\Omega,\ t>0,\\
q_t = bu-\gamma q, & x\in\Omega,\ t>0,\\
\partial_n u = \partial_n v = 0, & x\in\partial\Omega,\ t>0,
\end{cases}
\tag{1.4}
$$

where the growth of $q(x,t)$ follows a constant proportion $b>0$ to resource density, and $q(x,t)$ has a linear decay at rate $\gamma>0$.

When $q(x,t)$ satisfies (H2), Eq.(1.2) becomes the following system:

$$
\begin{cases}
u_t = d_1\Delta u + u\left(1-\dfrac{u}{k}\right) - \dfrac{muv}{1+u}, & x\in\Omega,\ t>0,\\
v_t = d_2\Delta v - \chi\nabla\cdot(v\nabla q) + \dfrac{muv}{1+u} - dv, & x\in\Omega,\ t>0,\\
q_t = buv-(\gamma+\xi v)q, & x\in\Omega,\ t>0,\\
\partial_n u = \partial_n v = 0, & x\in\partial\Omega,\ t>0.
\end{cases}
\tag{1.5}
$$

The difference between model (1.4) and model(1.5) is that $q(x,t)$ in (1.5) grows proportionally both to the resource and consumer density, $q(x,t)$ in (1.4) depends only on the resource. The assumption in model(1.5) is more reasonable because spatial memory is normally gained via interactive learning. Consumers may be able to share knowledge between individuals such that a location with high resource density is more likely to be remembered by consumers. In addition to a linear decay, we assume that $q(x,t)$ can further decay at rate $\xi>0$ when the consumers return to an area and find a low resource density.

For $\chi\in\mathbb{R},\ \gamma>0$, our main results are stated as follows:

1. The spectrum of the linearized operator at the constant steady state of system (1.4)/(1.5) is point spectrum, and the stability of the constant steady state is determined by the linearized eigenvalue problem (2.7)/(3.3).
2. In system (1.4), there exist $\chi_N^S<0$ and $\chi_M^S>0$, such that the constant steady state is stable when the memory-based diffusion rate $\chi\in(\chi_N^S(\gamma),\chi_M^H(\gamma))$ and unstable when $\chi\in(-\infty,\chi_N^S(\gamma))\cup(\chi_M^H(\gamma),+\infty)$, where $\chi_N^S(\gamma)<0$ and $\chi_M^H(\gamma)>0$ are the maximum steady state bifurcation value and the minimum Hopf bifurcation value, respectively. A series of steady-state bifurcations can occur near the constant steady state at $\chi=\chi_n^S(\gamma)<0$, and Hopf bifurcations occur at $\chi_n^H(\gamma)>0$ for $n\in\mathbb{N}$.
3. In system (1.5), there exist $\chi^-(\gamma)<0$ and $\chi^+(\gamma)>0$, such that the constant steady state is stable when the memory-based diffusion rate $\chi\in(\chi^-(\gamma),\chi^+(\gamma))$ and unstable when $\chi\in(-\infty,\chi^-(\gamma))\cup(\chi^+(\gamma),+\infty)$, where $\chi^-(\gamma)=\tilde\chi_N^S(\gamma),\ \chi^+(\gamma)=\min\left\{\tilde\chi_M^H(\gamma),\tilde\chi_\infty^S(\gamma)\right\}$ and $\tilde\chi_N^S(\gamma)<0,\ \tilde\chi_M^H(\gamma)>0,\ \tilde\chi_\infty^S(\gamma)>0$ are constants defined in Sect.3. A series of steady-state bifurcations can occur near the constant steady state at $\chi=\chi_n^S(\gamma)$, and Hopf bifurcations occur at $\chi_n^H(\gamma)>0$ for $n\in\mathbb{N}$. Note that $\chi_n^S(\gamma)$ could be negative or positive for different $n\in\mathbb{N}$.

This paper is organized as follows. We investigate the dynamics and bifurcation of system (1.4) in Sect.2 with a description of the spectrum of the linearized operator at the constant steady state. In Sect.3, system (1.5) is investigated similarly to in Sect.2. Finally, we conclude and discuss our work in Sect.4 and compare the two models studied in Sects.2 and 3. In the paper the space of measurable functions for which the p-th power of the absolute value is Lebesgue integrable defined on a bounded and smooth domain $\Omega \subseteq \mathbb{R}^m$ is denoted by $L^p(\Omega)$ and we use $W^{k,p}(\Omega)$ to denote the real-valued Sobolev space based on $L^p(\Omega)$ space. We denote by $\mathbb{N}$ the set of all the positive integers and $\mathbb{N}_0 = \mathbb{N} \cup \{0\}$. Also, λ_n satisfying $0 = \lambda_0 < \lambda_1 < \cdots < \lambda_{n-1} < \lambda_n < \cdots < +\infty$ are the eigenvalues of the following equation

$$\begin{cases} \Delta\phi(x) + \lambda\varphi(x) = 0, & x \in \Omega, \\ \partial_n \phi(x) = 0, & x \in \partial\Omega, \end{cases}$$

with the corresponding eigenfunctions $\phi_n(x) > 0$ satisfying $\int_\Omega \phi_n^2(x)dx = 1$.

2. The dynamics of model (1.4). In this section, we study the dynamics of system (1.2) with cognitive map $q(x,t)$ satisfying (H1), i.e. model (1.4), which has a constant equilibrium $(u, v, q) = (\theta, v_\theta, q_\theta)$ with

$$\theta = \frac{d}{m-d},\ v_\theta = \frac{(k-\theta)(1+\theta)}{km},\ q_\theta = \frac{b\theta}{\gamma},$$

provided that

$$m > d,\ k > \theta. \tag{2.1}$$

By a standard calculation, the linearized Jacobian matrix of the kinetic system of (1.4) at $(\theta, v_\theta, q_\theta)$ is

$$J = \begin{pmatrix} \beta & -d & 0 \\ \alpha & 0 & 0 \\ b & 0 & -\gamma \end{pmatrix},$$

where

$$\alpha = \frac{k-\theta}{k(1+\theta)} > 0,\ \beta = \frac{\theta(k-1-2\theta)}{k(1+\theta)} < 0. \tag{2.2}$$

One can easily verify that all the eigenvalues of J have negative real parts when $k < 1 + 2\theta$ such that $(\theta, v_\theta, q_\theta)$ is locally asymptotically stable concerning the kinetic system. Note that $k = 1 + 2\theta$ is the critical value for the kinetic system to undergo a Hopf bifurcation near $(\theta, v_\theta, q_\theta)$. Together with (2.1), we always assume the following conditions hold:

(A) $m > d,\ \theta < k < 1 + 2\theta$,

such that $(\theta, v_\theta, q_\theta)$ is locally asymptotically stable concerning the kinetic system.

In the following, we investigate the stability of the constant steady state $(\theta, v_\theta, q_\theta)$ and carry a bifurcation analysis for system (1.4). Moreover, we will show the existence of nonconstant positive steady states of model (1.4), which satisfy

$$\begin{cases} d_1 \Delta u + u\left(1 - \frac{u}{k}\right) - \frac{muv}{1+u} = 0, & x \in \Omega, \\ d_2 \Delta v - \chi \nabla \cdot (v \nabla q) + \frac{muv}{1+u} - dv = 0, & x \in \Omega, \\ bu - \gamma q = 0, & x \in \Omega, \\ \partial_n u = \partial_n v = 0, & x \in \partial\Omega, \end{cases} \tag{2.3}$$

where $u = u(x),\ v = v(x),\ q = q(x)$.

2.1. Spectrum of the linearized operator. In this part, we perform a spectral analysis of the linearized operator at the constant steady state $(\theta, v_\theta, q_\theta)$ via the methods in [3, 13, 15]. Define

$$X = W_N^{2,p}(\Omega) \times W_N^{2,p}(\Omega) \times W^{2,p}(\Omega),\ Y = L^p(\Omega) \times L^p(\Omega) \times L^p(\Omega), \tag{2.4}$$

where

$$W_N^{2,p}(\Omega) = \{u \in W^{2,p}(\Omega) : \partial_n u = 0 \text{ on } \partial\Omega\}.$$

We linearize Eq.(1.4) at $(\theta, v_\theta, q_\theta)$ and obtain the linear operator

$$\mathcal{L}\begin{pmatrix}\phi\\ \psi\\ \varphi\end{pmatrix} = \begin{pmatrix} d_1\Delta\phi + \beta\phi - d\psi \\ d_2\Delta\psi - \chi v_\theta \Delta\varphi + \alpha\phi \\ b\phi - \gamma\varphi \end{pmatrix}, \tag{2.5}$$

where $\mathcal{L}$ is a closed linear operator in Y with domain $D(\mathcal{L}) = X$. In the following, we provide the results about the spectrum of $\mathcal{L}$.

Theorem 2.1. *Let $\mathcal{L} : X \to Y$ be defined as (2.5), then the spectrum of $\mathcal{L}$ is*

$$\sigma(\mathcal{L}) = \sigma_p(\mathcal{L}) = S \cup \{-\gamma\},$$

where

$$S = \{\mu_n^{(1)}\}_{n=0}^\infty \cup \{\mu_n^{(2)}\}_{n=0}^\infty \cup \{\mu_n^{(3)}\}_{n=0}^\infty. \tag{2.6}$$

Here $\mu_n^{(j)},\ j = 1, 2, 3$ satisfying $\mathcal{R}e\left(\mu_n^{(1)}\right) < \mathcal{R}e\left(\mu_n^{(2)}\right) < \mathcal{R}e\left(\mu_n^{(3)}\right)$ are the roots of the following characteristic equation

$$\mu^3 + A_n\mu^2 + B_n\mu + C_n = 0,\quad n \in \mathbb{N}_0, \tag{2.7}$$

where

$$\begin{aligned} A_n &= (d_1 + d_2)\lambda_n - \beta + \gamma,\\ B_n &= d_2\lambda_n(d_1\lambda_n - \beta) + \gamma(d_1\lambda_n + d_2\lambda_n - \beta) + d\alpha,\\ C_n &= \gamma d_2\lambda_n(d_1\lambda_n - \beta) + bd\chi v_\theta\lambda_n + \gamma d\alpha. \end{aligned}$$

Proof. For $\mu \in \mathbb{C}$ and $(\tau_1, \tau_2, \tau_3) \in Y$, we consider the nonhomogeneous problem

$$\begin{cases} d_1\Delta\phi + \beta\phi - d\psi = \mu\phi + \tau_1,\\ d_2\Delta\psi - \chi v_\theta\Delta\varphi + \alpha\phi = \mu\psi + \tau_2,\\ b\phi - \gamma\varphi = \mu\varphi + \tau_3,\\ \partial_n\phi = \partial_n\psi = 0. \end{cases} \tag{2.8}$$

Case 1: $\mu \neq -\gamma$. From the third equation of (2.8), we obtain $\varphi = \dfrac{b\phi - \tau_3}{\mu + \gamma}$ and substitute it into the second equation, we have

$$\begin{cases} d_1\Delta\phi + \beta\phi - d\psi = \mu\phi + \tau_1,\\ d_2\Delta\psi - \dfrac{\chi v_\theta}{\mu + \gamma}(b\Delta\phi - \Delta\tau_3) + \alpha\phi = \mu\psi + \tau_2,\\ \partial_n\phi = \partial_n\psi = 0, \end{cases} \tag{2.9}$$

which is equivalent to

$$\mathcal{L}_1\begin{pmatrix}\phi\\ \psi\end{pmatrix}=\begin{pmatrix} d_1\Delta\phi+\beta\phi-d\psi-\mu\phi\\ d_2\Delta\psi-\dfrac{b\chi v_\theta}{\mu+\gamma}\Delta\phi+\alpha\phi-\mu\psi\end{pmatrix}=\begin{pmatrix}\tau_1\\ \tau_2-\dfrac{\chi v_\theta}{\mu+\gamma}\Delta\tau_3\end{pmatrix}. \tag{2.10}$$

As $\phi,\ \psi\in W_N^{2,p}(\Omega)$ from (2.5), and the eigenfunctions $\{\phi_n\}_{n=0}^{+\infty}$ of $-\Delta$ form a complete and orthonormal basis for $W_N^{2,p}(\Omega)$, thus we set

$$\phi=\sum_{n=0}^{+\infty}a_n\phi_n,\ \ \psi=\sum_{n=0}^{+\infty}b_n\phi_n. \tag{2.11}$$

Substituting (2.11) into (2.10), multiplying the equation by ϕ_n and integrating it over Ω, we obtain

$$\begin{pmatrix}-d_1\lambda_n+\beta-\mu & -d\\ \dfrac{b\chi v_\theta\lambda_n}{\mu+\gamma}+\alpha & -d_2\lambda_n-\mu\end{pmatrix}\begin{pmatrix}a_n\\ b_n\end{pmatrix}=\begin{pmatrix}\displaystyle\int_\Omega\tau_1dx\\ \displaystyle\int_\Omega\left(\tau_2-\dfrac{\chi v_\theta}{\mu+\gamma}\Delta\tau_3\right)dx\end{pmatrix}.$$

By letting $\tau_1=\tau_2=\tau_3=0$, we obtain that $Ker(\mathcal{L}_1)=\{(0,0)^T\}$ which implies that $Ker(\mathcal{L}-\mu I)=\{(0,0,0)^T\}$ and the operator $\mathcal{L}-\mu I$ is injective when the following condition holds

$$\begin{vmatrix}-d_1\lambda_n+\beta-\mu & -d\\ \dfrac{b\chi v_\theta\lambda_n}{\mu+\gamma}+\alpha & -d_2\lambda_n-\mu\end{vmatrix}\neq 0,$$

which is equivalent to

$$(\mu+d_1\lambda_n-\beta)(\mu+d_2\lambda_n)(\mu+\gamma)+bd\chi v_\theta\lambda_n\neq 0. \tag{2.12}$$

When (2.12) is satisfied, we may conclude that $\mathcal{L}_1$ has a bounded inverse $\mathcal{L}_1^{-1}$ with

$$\begin{aligned}&\|\phi\|_{W^{2,p}(\Omega)}+\|\psi\|_{W^{2,p}(\Omega)}\\ \leq&\|\mathcal{L}_1^{-1}\|\left(\|d_1\Delta\phi+\beta\phi-d\psi\|_{L^p(\Omega)}+\left\|d_2\Delta\psi-\frac{b\chi v_\theta}{\mu+\gamma}\Delta\phi+\alpha\phi\right\|_{L^p(\Omega)}\right).\end{aligned}$$

Therefore, we know that $\mathcal{L}-\mu I$ has a bounded inverse $(\mathcal{L}-\mu I)^{-1}$.

If (2.12) does not hold, that is,

$$\begin{vmatrix}-d_1\lambda_n+\beta-\mu & -d\\ \dfrac{b\chi v_\theta\lambda_n}{\mu+\gamma} & -d_2\lambda_n-\mu\end{vmatrix}=0, \tag{2.13}$$

we obtain the dispersal relation as in (2.7) which has three roots $\mu_n^{(j)},\ j=1,2,3$ for each $n\in\mathbb{N}_0$. For $j=1,2,3$, we put $\mu=\mu_n^{(j)}$ into (2.8), one can check that $\mu_n^{(j)}$ are indeed eigenvalues of $\mathcal{L}$ with eigenfunctions being

$$\begin{pmatrix}\phi_n^{(j)}\\ \psi_n^{(j)}\\ \varphi_n^{(j)}\end{pmatrix}=\begin{pmatrix}1\\ \dfrac{1}{d}\left(-d_1\lambda_n+\beta-\mu_n^{(j)}\right)\\ \dfrac{b}{\mu_n^{(j)}+\gamma}\end{pmatrix}\phi_n,$$

which implies that $Ker(\mathcal{L}-\mu_n^{(j)}) = Span\left\{\left(\phi_n^{(j)}, \psi_n^{(j)}, \varphi_n^{(j)}\right)^T\right\}$.

Case 2: $\mu = -\gamma$. Then Eq. (2.8) becomes

$$\begin{cases} d_1\Delta\phi + \beta\phi - d\psi = \mu\phi + \tau_1, \\ d_2\Delta\psi - \chi v_\theta \Delta\varphi + \alpha\phi = \mu\psi + \tau_2, \\ b\phi = \tau_3, \\ \partial_n\phi = \partial_n\psi = 0, \end{cases} \tag{2.14}$$

which can be solved as

$$\begin{cases} \psi = \dfrac{1}{bd}\left(d_1\Delta\tau_3 + \beta\tau_3 + \gamma\tau_3 - b\tau_1\right), \\ \Delta\varphi = \dfrac{1}{b\chi v_\theta}\left(-b\gamma\psi + \tau_2 - \alpha\tau_3 - bd_2\Delta\psi\right). \end{cases}$$

By letting $\tau_1 = \tau_2 = \tau_3 = 0$, we obtain $Ker\left(\mathcal{L}+\gamma I\right) = Span\{(0, 0, c_1x + c_2)^T\}$ with $c_1,\ c_2$ being constant real numbers, and thus $-\gamma \in \sigma_p(\mathcal{L})$. To conclude, we have

$$\sigma(\mathcal{L}) = \sigma_p(\mathcal{L}) = S \cup \{-\gamma\}$$

with S defined as (2.6). This completes the proof. ∎

Based on the spectrum analysis in Theorem 2.1, we obtain the following results to determine the stability of the constant equilibrium for Eq. (1.4).

COROLLARY 2.2. *In system* (1.4)*, the constant equilibrium* $(\theta, v_\theta, q_\theta)$ *is locally stable when all the roots of the characteristic equation* (2.7) *have negative real parts, otherwise it is unstable.*

Proof. From Theorem 2.1, we see that the spectrum of the linearized operator $\mathcal{L}$ corresponding to the linearized system of Eq. (1.4) at $(\theta, v_\theta, q_\theta)$ is $\sigma(\mathcal{L}) = \sigma_p(\mathcal{L}) = S \cup \{-\gamma\}$. Note that the linear stability of $(\theta, v_\theta, q_\theta)$ implies its nonlinear stability according to [9] as the spectral set is discrete. Since $-\gamma \in \mathbb{C}^-$, thus it can be inferred that the stability of $(\theta, v_\theta, q_\theta)$ is determined by the set S which consists of the roots of Eq. (2.7), and we reach our conclusion. ∎

2.2. Bifurcation analysis. From Theorem 2.1 and Corollary 2.2, we know that the stability of the constant steady state $(\theta, v_\theta, q_\theta)$ of system (1.4) can be determined by the characteristic equation (2.7). By the Routh-Hurwitz stability criterion, all the eigenvalues of (2.7) have negative real parts if and only if

$$A_n > 0,\ \ C_n > 0,\ \ A_nB_n - C_n > 0. \tag{2.15}$$

The condition $A_n > 0$ always holds as $\beta < 0$, thus the real parts of the eigenvalues of (2.7) may change sign either via $C_n = 0$ (which implies (2.7) has a zero root) or via $A_nB_n - C_n = 0$ (which implies (2.7) has a pair of purely imaginary roots). Also, we can observe that $B_n > 0$ always holds as $\beta < 0,\ \alpha > 0$, so $C_n = 0$ and $A_nB_n - C_n = 0$ cannot occur at the same time.

Taking χ and γ as the bifurcation parameters, we obtain the steady-state bifurcation points by solving $C_n = 0$:

$$\chi_n^S(\gamma) = -\frac{\gamma k d_2\lambda_n(d_1\lambda_n - \beta) + \gamma d\alpha}{bdv_\theta\lambda_n}, \tag{2.16}$$

and Hopf bifurcation points by solving $A_nB_n - C_n = 0$:

(2.17)
$$\chi_n^H(\gamma) = \frac{((d_1+d_2)\lambda_n - \beta)\left[\gamma^2 + \gamma((d_1+d_2)\lambda_n - \beta) + d_2\lambda_n(d_1\lambda_n - \beta) + d\alpha\right]}{bdv_\theta\lambda_n}.$$

Some basic properties of functions $\chi_n^S(\gamma)$ and $\chi_n^H(\gamma)$ are stated in the following lemma.

Lemma 2.3. *Let $\chi_n^S(\gamma)$ and $\chi_n^H(\gamma)$ be defined as (2.16) and (2.17), respectively, then the following statements are true:*

(i) for fixed n, $\chi_n^S(\gamma)$ is strictly decreasing with respect to γ and passes through the origin, and it is also known that $\chi_n^S(0) = 0$ and $\lim_{\gamma\to+\infty} \chi_n^S(\gamma) = -\infty$;

(ii) for fixed $\gamma > 0$, $\chi_N^S(\gamma) = \max_{n\in\mathbb{N}} \chi_n^S(\gamma)$, and

$$\chi_N^S(\gamma) < -\frac{\left(2\sqrt{d_1d_2d\alpha} - d_2\beta\right)\gamma}{bdv_\theta}, \tag{2.18}$$

where N is an integer such that λ_N is the closest number to $\sqrt{\frac{d\alpha}{d_1d_2}}$;

(iii) for fixed $n \in \mathbb{N}$, $\chi_n^H(\gamma)$ is strictly increasing with respect to γ;

(iv) for fixed $\gamma \in (0, +\infty)$, there exists $M \in \mathbb{N}$ such that $\chi_M^H(\gamma) = \min_{n\in\mathbb{N}} \chi_n^H(\gamma)$.

Proof. By the definition of $\chi_n^S(\gamma)$ given in (2.16), it is easy to see that $\chi_n^S(\gamma)$ is a straight line passing through the origin with the slope

$$K_n = -\frac{1}{bdv_\theta}\left(d_1d_2\lambda_n + \frac{d\alpha}{\lambda_n} - d_2\beta\right) < 0,$$

then we immediately obtain the results in (i). Also, we see that K_n is a hook function of λ_n, thus it can be known that K_n reaches its maximum at $\lambda_n = \sqrt{\frac{d\alpha}{d_1d_2}}$, thus the conclusion in (ii) is achieved.

For (iii), it is clear from (2.17) that $\chi_n^H(\gamma)$ is a quadratic function of γ and can be rewritten as $\chi_n^H(\gamma) = a_2\gamma^2 + a_1\gamma + a_0$ with

$$\begin{aligned} a_2 &= \frac{(d_1+d_2)\lambda_n - \beta}{bdv_\theta\lambda_n},\ a_1 = \frac{((d_1+d_2)\lambda_n - \beta)^2}{bdv_\theta\lambda_n}, \\ a_0 &= \frac{((d_1+d_2)\lambda_n - \beta)d_2\lambda_n(d_1\lambda_n - \beta) + d\alpha}{bdv_\theta\lambda_n}. \end{aligned}$$

Immediately, we obtain that $a_2 > 0,\ a_1 > 0,\ a_0 > 0$ and the symmetrical axis $\gamma = -\frac{a_1}{2a_2} < 0$. Thus, it can be inferred that $\chi_n^H(\gamma)$ is increasing for $\gamma > 0$.

For (iv), we first rewrite $\chi_n^H(\gamma)$ as the following form by replacing λ_n by a continuous variable p:

$$\chi_p^H(\gamma) = \frac{((d_1+d_2)p - \beta)\left[\gamma^2 + \gamma(d_1p + d_2p - \beta) + d_2p(d_1p - \beta) + d\alpha\right]}{bdv_\theta p}. \tag{2.19}$$

By differentiating $\chi_p^H(\gamma)$ with respect to p, we have

$$\begin{aligned} \frac{d[\chi_p^H(\gamma)]}{dp} =& \frac{1}{bdv_\theta p^2}\left[2(d_1+d_2)d_1d_2p^3 + ((d_1+d_2)^2\gamma\right. \\ &\left. -\beta(2d_1d_2 + d_2^2))p^2 + \beta\gamma^2 - \beta^2\gamma + \beta d\alpha\right]. \end{aligned}$$

Let

$$f(p) = 2(d_1+d_2)d_1d_2p^3 + ((d_1+d_2)^2\gamma - \beta(2d_1d_2+d_2^2))p^2 + \beta\gamma^2 - \beta^2\gamma + \beta d\alpha,$$

then one can verify that $f(p)$ has a unique positive zero $p = p_*$ as

$$f'(p) = 6(d_1+d_2)d_1d_2p^2 + 2((d_1+d_2)^2\gamma - \beta(2d_1d_2+d_2^2))p > 0, \text{ for } p > 0,$$

and $f(0) = \beta\gamma^2 - \beta^2\gamma + \beta d\alpha < 0$, $\lim\limits_{p\to+\infty} f(p) = +\infty$. Also we found that $f(p) > 0$ for $p \in (p_*, +\infty)$ and $f(p) < 0$ for $p \in (0, p_*)$, which implies that $\dfrac{d[\chi_p^H(\gamma)]}{dp} > 0$ for $p \in (p_*, +\infty)$ and $\dfrac{d[\chi_p^H(\gamma)]}{dp} < 0$ for $p \in (0, p_*)$ and $\chi_p^H(\gamma)$ reaches its minimum at $p = p_*$. By the relation that $p = \lambda_n$, we know that there must exist a $M \in \mathbb{N}$ such that λ_M is the closest eigenvalue to p_* and $\chi_M^H(\gamma) = \min\limits_{n\in\mathbb{N}} \chi_n^H(\gamma)$. ∎

LEMMA 2.4. *Let $\chi_N^S(\gamma)$ and $\chi_M^H(\gamma)$ be defined as in Lemma 2.3, then we have*
(i) *when $\chi_N^S(\gamma) < \chi < \chi_M^H(\gamma)$, all the eigenvalues of Eq.(2.7) have negative real parts;*
(ii) *when $\chi \geq \chi_M^H(\gamma)$, $\mu = \pm i\omega_n$ $(\omega_n > 0)$ is a pair of purely imaginary roots of Eq.(2.7) if $\chi = \chi_n^H(\gamma)$;*
(iii) *when $\chi \leq \chi_N^S(\gamma)$, $\mu = 0$ is a root of Eq. (2.7) if $\chi = \chi_n^S(\gamma)$.*

Proof. From Lemma 2.3, when $\chi_N^S(\gamma) < \chi < \chi_M^H(\gamma)$, we have $C_n > 0$ and $A_nB_n - C_n > 0$ for all $\lambda_n > 0$ so all the eigenvalues of (2.7) have negative real parts for all $n \in \mathbb{N}_0$. When $\chi \leq \chi_N^S(\gamma)$, we have $C_n < 0$ so the characteristic equation (2.7) has at least one eigenvalue with positive real part, and when $\chi = \chi_n^S(\gamma)$, Eq.(2.7) has a zero eigenvalue. When $\chi \geq \chi_M^H(\gamma)$, we have $A_n > 0$, $C_n > 0$ but $A_nB_n - C_n < 0$, so not all the eigenvalues of (2.7) have negative real parts. In particular, when $\chi = \chi_n^H(\gamma)$, Eq.(2.7) has a pair of complex eigenvalues with zero real part. ∎

From Lemma 2.4, we know that Eq.(2.7) has a pair of purely imaginary eigenvalues $\pm i\omega_n$ $(\omega_n > 0)$ when $\chi = \chi_n^H(\gamma)$. The following lemma shows that the transversality condition holds at $\chi = \chi_n^H(\gamma)$.

LEMMA 2.5. *Let $\chi = \chi_n^H(\gamma)$ be defined as (2.17). Then, Eq.(2.7) has a pair of roots in the form of $\mu = \delta(\chi) \pm i\omega(\chi)$ when χ is near $\chi_n^H(\gamma)$ such that $\delta\left(\chi_n^H(\gamma)\right) = 0$ and $\delta'\left(\chi_n^H(\gamma)\right) > 0$.*

Proof. We only need to show that $\delta'\left(\chi_n^H(\gamma)\right) > 0$. Differentiating Eq.(2.7) with respect to χ, we have

$$3\mu^2\frac{d\mu}{d\chi} + \frac{dA_n}{d\chi}\mu^2 + 2A_n\mu\frac{d\mu}{d\chi} + \frac{dB_n}{d\chi}\mu + B_n\frac{d\mu}{d\chi} + \frac{dC_n}{d\chi} = 0. \tag{2.20}$$

From the expressions of A_n, B_n, C_n in Eq. (2.7), it is straightforward to see that

$$\frac{dA_n}{d\chi} = 0, \ \frac{dB_n}{d\chi} = 0, \ \frac{dC_n}{d\chi} = bdv_\theta\lambda_n. \tag{2.21}$$

Substituting (2.21), $\mu = i\omega_0$, $B_n = \omega_0^2$ and $\chi = \chi_n^H(\gamma)$ into Eq. (2.20), we obtain

$$\left.\frac{d\mu}{d\chi}\right|_{\chi=\chi_n^H(\gamma)} = \frac{bdv_\theta\lambda_n}{2\omega_0^2 - 2i\omega_0A_n},$$

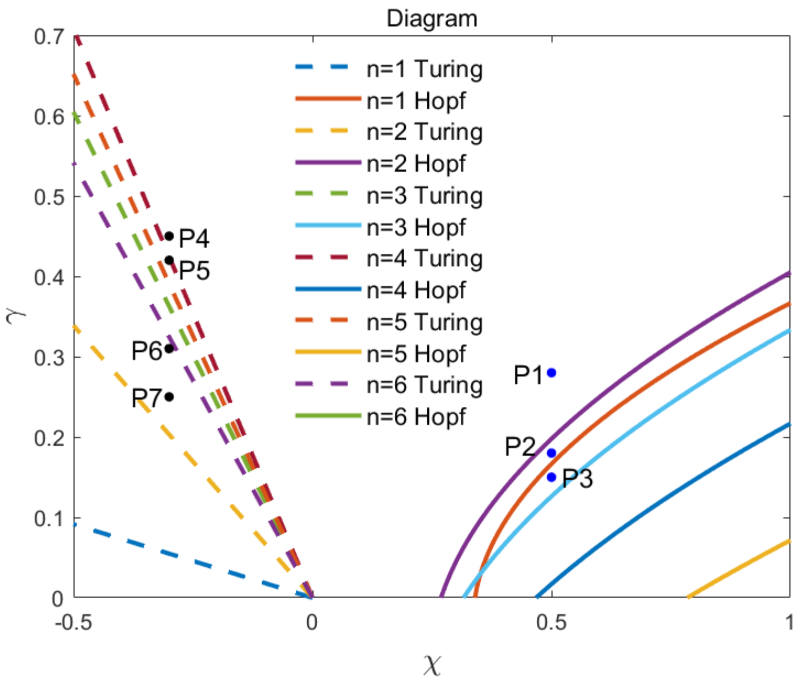

Fig. 1: The bifurcation diagram of system (1.4) in (χ, γ) plane with $d_1 = 0.01,\ d_2 = 0.03,\ m = 1,\ d = 0.1,\ k = 1,\ b = 0.15,\ \Omega = (0, \pi)$, and the Turing bifurcation curves $\chi = \chi_n^S(\gamma)$ can be identified by the dotted curves and Hopf bifurcation curves $\chi = \chi_n^H(\gamma)$ by the solid curves. The points are parameter values for the numerical simulations and they are: P1 $(0.5, 0.28)$, P2 $(0.5, 0.18)$, P3 $(0.5, 0.15)$, P4 $(-0.3, 0.45)$, P5 $(-0.3, 0.42)$, P6 $(-0.3, 0.31)$ and P7 $(-0.3, 0.25)$.

thus

$$\delta'(\chi) = \mathcal{R}e\left(\frac{d\mu}{d\chi}\Big|_{\chi=\chi_n^H(\gamma)}\right) = \frac{bdv_\theta\lambda_n}{2(\omega_0^2 + A_n^2)} > 0.$$

$\square$

By Lemmas 2.3, 2.4, 2.5 and Hopf bifurcation theory for partial functional differential equations, we obtain the following results on the stability and bifurcation behaviors of the positive homogeneous steady state of Eq.(1.4).

Theorem 2.6. *Assume that condition (A) holds, and let $\chi_n^S(\gamma),\ \chi_n^H(\gamma)$ be defined as* (2.16), (2.17) *and $\chi_N^S(\gamma), \chi_M^H(\gamma)$ in Lemma 2.3, then we have the following results for Eq.*(1.4)*:*

(i) a mode-n Turing bifurcation occurs at $\chi = \chi_n^S(\gamma)$ for $\gamma > 0$ and $n \in \mathbb{N}$, thus a mode-n spatially nonhomogeneous steady state can arise near $(\theta, v_\theta, q_\theta)$;

(ii) a mode-n Hopf bifurcation occurs at $\chi = \chi_n^H(\gamma)$ for $\gamma > 0$ and $n \in \mathbb{N}$, and the bifurcating periodic solutions are spatially nonhomogeneous;

(iii) for a fixed $\gamma \in (0, +\infty)$, the positive homogeneous steady state $(\theta, v_\theta, q_\theta)$ is locally asymptotically stable for $\chi_N^S(\gamma) < \chi < \chi_M^H(\gamma)$ and unstable for $\chi \in \left(-\infty, \chi_N^S(\gamma)\right] \cup \left[\chi_M^H(\gamma), +\infty\right)$.

On one-dimension spatial domain $\Omega = (0, \pi)$, the bifurcation diagram of Eq.(1.4) is illustrated in Fig.1 by taking the parameters as $d_1 = 0.01,\ d_2 = 0.03,\ m = 1,\ d = 0.1,\ k = 1,\ b = 0.15$. In the following, we perform some numerical simulations based on the following initial conditions:

(I1) $u_0(x) = \theta - 0.01\cos(x),\ v_0(x) = v_\theta - 0.01\cos(x),\ q_0(x) = q_\theta - 0.1\cos(x)$,
(I2) $u_0(x) = \theta - 0.01\cos(2x),\ v_0(x) = v_\theta - 0.01\cos(2x),\ q_0(x) = q_\theta - 0.1\cos(2x)$,
(I3) $u_0(x) = \theta - 0.01\cos(3x),\ v_0(x) = v_\theta - 0.01\cos(3x),\ q_0(x) = q_\theta - 0.1\cos(3x)$,
(I4) $u_0(x) = \theta - 0.01\cos(4x),\ v_0(x) = v_\theta - 0.01\cos(4x),\ q_0(x) = q_\theta - 0.1\cos(4x)$,

and we will indicate the initial conditions for each figure. Note that we only demonstrate the distribution of resources in each figure as the consumers always follow the resources and have similar spatial distribution.

From Fig.1, we observe that the mode-2 Hopf curve is the first Hopf curve and we choose some points near the Hopf bifurcation curves to observe periodic patterns in system (1.4). In Fig.2, for fixed $\chi = 0.5$, we observe that the steady state $(\theta, v_\theta, q_\theta)$ is stable when $\gamma = 0.28$ (corresponding to P1 which is in the stable region). When we decrease γ to 0.18 (corresponding to P2 which is under the first Hopf bifurcation curve), it is shown that a mode-2 spatially nonhomogeneous periodic pattern arises. When $\gamma = 0.15$, the mode-2 spatially nonhomogeneous periodic pattern remains stable as the mode-2 Hopf bifurcation curve is the dominant Hopf bifurcation curve. Also, if the initial conditions are taken as **(I1)** and **(I3)**, the solution of system (1.4) finally converges to a mode-2 periodic pattern but with a transient oscillation between different modes, see Fig.3. In this situation, we see that the spatial distribution of resources will periodically change over time.

In Fig.4, we demonstrate the spatially nonhomogeneous steady state and some wandering periodic patterns when $\chi = -0.3$. When we choose $\gamma = 0.45$ corresponding to P4 in Fig.1, the constant steady state $(\theta, v_\theta, q_\theta)$ is stable as shown in (a). If we decrease γ to 0.42 corresponding to P5 which is below the mode-4 Turing curve, it is shown that a mode-4 spatially nonhomogeneous steady state arises as illustrated in (b). This situation happens when the environment of the living habitat is steady over time so that resources and consumers can keep their dynamic balance. When we continue to decrease the γ value, we observe some "wandering" patterns with large periods as shown in (c) and (d), which demonstrate a distinguished distribution of resources from the periodic patterns (see Fig.2) induced by Hopf bifurcation. These patterns are also observed in previous work of Keller–Segel chemotaxis model with growth [19] and distributed spatial memory [27]. The mechanism behind these patterns is to be explored, while it is sure that Hopf bifurcation from a constant steady state is not the reason as we have proved that Hopf bifurcation will not occur in the parameter region where we observe these "wandering" patterns.

3. The dynamics of model (1.5).

In this section, we investigate the dynamics of system (1.5), which admits a constant equilibrium $(\theta, v_\theta, \tilde{q}_\theta)$ with

$$\theta = \frac{d}{m-d},\ v_\theta = \frac{(k-\theta)(1+\theta)}{km},\ \tilde{q}_\theta = \frac{b\theta v_\theta}{\gamma + \xi v_\theta}.$$

One can easily verify that $(\theta, v_\theta, q_\theta)$ is locally asymptotically stable concerning the kinetic system. In this section, we investigate the stability of the constant steady state $(\theta, v_\theta, \tilde{q}_\theta)$ and carry a bifurcation analysis for system (1.5).

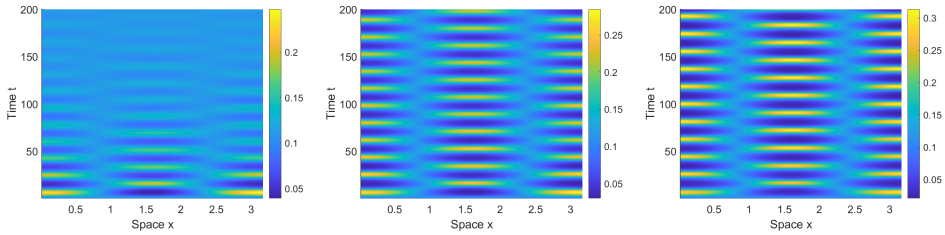

(a) $(\chi, \gamma) = P1$,IC=**(I2)** (b) $(\chi, \gamma) = P2$,IC=**(I2)** (c) $(\chi, \gamma) = P3$,IC=**(I2)**

Fig. 2: Periodic patterns rising near Hopf bifurcation curves in system (1.4) when parameters are $d_1 = 0.01$, $d_2 = 0.03$, $m = 1$, $d = 0.1$, $k = 1$, $b = 0.15$ and $\Omega = (0, \pi)$. In each figure, the color indicates the value of $u(x, t)$ according to the color bar.

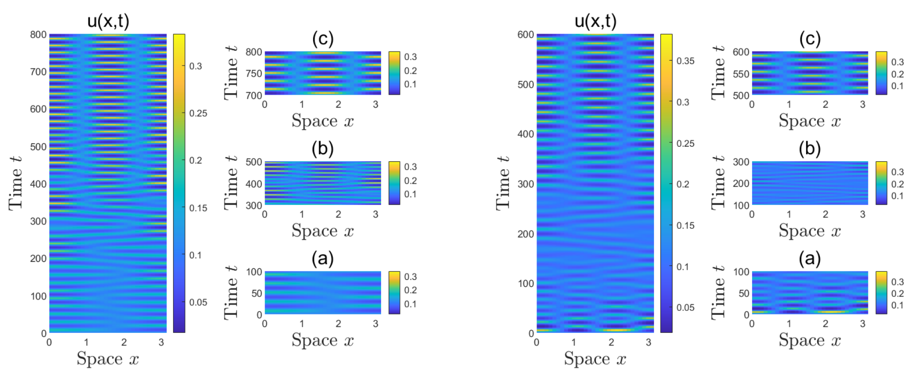

(a) $(\chi, \gamma) = P3$, IC=**(I1)** (b) $(\chi, \gamma) = P3$, IC=**(I3)**

Fig. 3: Transient oscillatory patterns between the different modes of periodic patterns in system (1.4) when parameters are $d_1 = 0.01$, $d_2 = 0.03$, $m = 1$, $d = 0.1$, $k = 1$, $b = 0.15$ and $\Omega = (0, \pi)$. In each figure, the color indicates the value of $u(x, t)$ according to the color bar.

3.1. Spectrum of the linearized operator. Linearizing Eq.(1.5) at $(\theta, v_\theta, \tilde{q}_\theta)$ leads to the linear operator

$$\tilde{\mathcal{L}} \begin{pmatrix} \phi \\ \psi \\ \varphi \end{pmatrix} = \begin{pmatrix} d_1 \Delta \phi + \beta \phi - d\psi \\ d_2 \Delta \psi - \chi v_\theta \Delta \varphi + \alpha \phi \\ b v_\theta \phi + \dfrac{b\theta\gamma}{\gamma + \xi v_\theta} \psi - (\gamma + \xi v_\theta) \varphi \end{pmatrix}, \tag{3.1}$$

where $\alpha > 0$, $\beta < 0$ defined as (2.2). Then, we know that $\tilde{\mathcal{L}}$ is a closed linear operator in Y with domain $D(\tilde{\mathcal{L}}) = X$ with X, Y defined as in (2.4). In the following, we provide the results about the spectrum of $\tilde{\mathcal{L}}$.

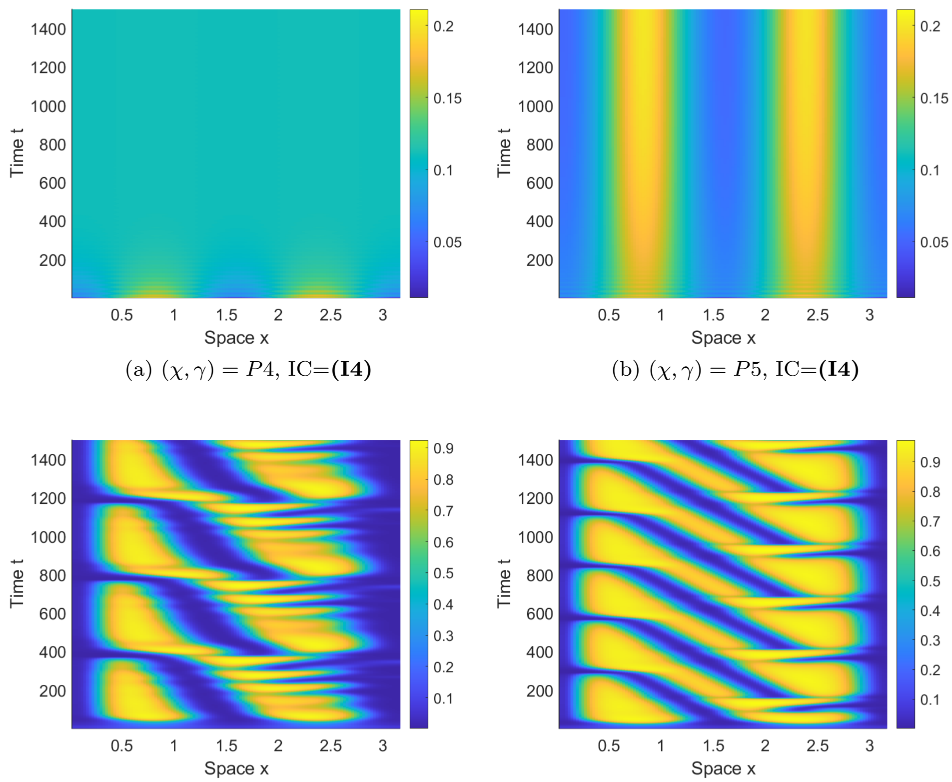

(a) $(\chi, \gamma) = P4$, IC=**(I4)**

(b) $(\chi, \gamma) = P5$, IC=**(I4)**

(c) $(\chi, \gamma) = P6$, IC=**(I4)**

(d) $(\chi, \gamma) = P7$, IC=**(I4)**

Fig. 4: Spatial patterns rising near Turing bifurcation curves in system (1.4) when parameters are $d_1 = 0.01,\ d_2 = 0.03,\ m = 1,\ d = 0.1,\ k = 1,\ b = 0.15$, and $\Omega = (0, \pi)$. In each figure, the color indicates the value of $u(x, t)$ according to the color bar.

THEOREM 3.1. *Let $\tilde{\mathcal{L}} : X \to Y$ be defined as (3.1), then the spectrum of $\tilde{\mathcal{L}}$ is*

$$\sigma\left(\tilde{\mathcal{L}}\right) = \sigma_p\left(\tilde{\mathcal{L}}\right) = \tilde{S} \cup \{-\gamma - \xi v_\theta\},$$

where

$$\tilde{S} = \{\tilde{\mu}_n^{(1)}\}_{n=0}^{\infty} \cup \{\tilde{\mu}_n^{(2)}\}_{n=0}^{\infty} \cup \{\tilde{\mu}_n^{(3)}\}_{n=0}^{\infty}, \tag{3.2}$$

where $\tilde{\mu}_n^{(j)},\ j = 1, 2, 3$ satisfying $\mathcal{R}e\left(\tilde{\mu}_n^{(1)}\right) < \mathcal{R}e\left(\tilde{\mu}_n^{(2)}\right) < \mathcal{R}e\left(\tilde{\mu}_n^{(3)}\right)$ are the roots of the following characteristic equation

$$\mu^3 + \tilde{A}_n \mu^2 + \tilde{B}_n \mu + \tilde{C}_n = 0, \quad n \in \mathbb{N}_0, \tag{3.3}$$

with

$$
\begin{aligned}
\tilde{A}_n &= (d_1+d_2)\lambda_n - \beta + \gamma + \xi v_\theta,\\
\tilde{B}_n &= d_2\lambda_n(d_1\lambda_n-\beta) + (\gamma+\xi v_\theta)(d_1\lambda_n + d_2\lambda_n - \beta) + \alpha - \frac{\chi b\theta v_\theta \gamma\lambda_n}{\gamma+\xi v_\theta},\\
\tilde{C}_n &= (\gamma+\xi v_\theta)d_2\lambda_n(d_1\lambda_n-\beta) + b\theta v_\theta^2\chi\lambda_n + d\alpha(\gamma+\xi v_\theta) - \frac{\chi b\theta v_\theta\gamma\lambda_n(d_1\lambda_n-\beta)}{\gamma+\xi v_\theta}.
\end{aligned}
$$

The proof of Theorem 3.1 is similar to that of Theorem 2.1, thus we put the details in Appendix.A.

COROLLARY 3.2. *In system (1.5), the constant equilibrium $(\theta, v_\theta, \tilde{q}_\theta)$ is locally stable when all the roots of the characteristic equation (3.3) have negative real parts; otherwise it is unstable.*

The proof is similar to that of Corollary 2.2, thus we omit it here.

3.2. Bifurcation analysis. From Theorem 3.1 and Corollary 3.2, we know that the stability of the constant steady state $(\theta, v_\theta, \tilde{q}_\theta)$ of system (1.5) can be determined by the characteristic equation (3.3). By the Routh-Hurwitz stability criterion, all eigenvalues of (3.3) have negative real parts if and only if

$$\tilde{A}_n > 0, \quad \tilde{C}_n > 0, \quad \tilde{A}_n\tilde{B}_n - \tilde{C}_n > 0.$$

From the fact that $\beta < 0$, we know that $\tilde{A}_n > 0$ always holds. Also we know that the real parts of the eigenvalues of (3.3) may change sign either via $\tilde{C}_n = 0$ (which implies (3.3) has a zero root) or via $\tilde{A}_n\tilde{B}_n - \tilde{C}_n = 0$ (which implies (3.3) has a pair of purely imaginary roots). Taking χ and γ as the bifurcation parameter, we obtain the steady state bifurcation points by solving $\tilde{C}_n = 0$:

$$\tilde{\chi}_n^S(\gamma) = -\frac{(\gamma+\xi v_\theta)(d_2\lambda_n(d_1\lambda_n-\beta)+d\alpha)}{bdv_\theta^2\lambda_n - (d_1\lambda_n-\beta)\frac{b\theta\gamma v_\theta\lambda_n}{\gamma+\xi v_\theta}}, \tag{3.4}$$

and Hopf bifurcation points by solving $\tilde{A}_n\tilde{B}_n - \tilde{C}_n = 0$:

$$
\begin{aligned}
\tilde{\chi}_n^H(\gamma) =& \frac{((d_1+d_2)\lambda_n-\beta)}{bdv_\theta^2\lambda_n + b\theta\gamma v_\theta\lambda_n + \frac{d_2 b\theta\gamma v_\theta\lambda_n^2}{\gamma+\xi v_\theta}}\left[d_2\lambda_n(d_1\lambda_n-\beta)\right.\\
&\left.+(\gamma+\xi v_\theta)((d_1+d_2)\lambda_n-\beta) + (\gamma+\xi v_\theta)^2 + d\alpha\right].
\end{aligned} \tag{3.5}
$$

In the following lemma, we give a detailed description of the properties of Turing curves $\chi = \tilde{\chi}_n^S(\gamma)$. For the convenience of writing, we define

$$
\begin{aligned}
Q_n(\gamma) &= (\gamma+\xi v_\theta)(d_2\lambda_n(d_1\lambda_n-\beta)+d\alpha),\\
P_n(\gamma) &= bdv_\theta^2\lambda_n - (d_1\lambda_n-\beta)\frac{b\theta\gamma v_\theta\lambda_n}{\gamma+\xi v_\theta}.
\end{aligned} \tag{3.6}
$$

LEMMA 3.3. *Let $\tilde{\chi}_n^S(\gamma)$ and $\tilde{\chi}_n^H(\gamma)$ be defined as (3.4) and (3.5), respectively, then the following statements are true:*

(i) there exists $n_* \in \mathbb{N}$ such that $\tilde{\chi}_n^S(\gamma) < 0$ for all $\gamma > 0$ when $n \le n_*$, and $\tilde{\chi}_n^S(\gamma) < 0$ for $\gamma \in (0, \gamma_n^*)$ and $\tilde{\chi}_n^S(\gamma) > 0$ for $\gamma \in (\gamma_n^*, +\infty)$ where γ_n^* satisfies $P_n(\gamma_n^*) = 0$ and n_* is the largest integer such that $\lambda_{n_*} < \dfrac{dv_\theta}{d_1\theta}$;

(ii) when $\tilde{\chi}_n^S(\gamma) < 0$, there exists $N \in \mathbb{N}$ such that $\tilde{\chi}_N^S = \max_{n\in\mathbb{N}} \tilde{\chi}_n^S$ for a fixed $\gamma > 0$;

(iii) when $\tilde{\chi}_n^S(\gamma) > 0$, $\tilde{\chi}_n^S$ is strictly decreasing with respect to n and satisfies

$$\tilde{\chi}_n^S > \tilde{\chi}_\infty^S = \frac{d_2(\gamma + \xi v_\theta)^2}{b\theta\gamma v_\theta}, \tag{3.7}$$

moreover, $\tilde{\chi}_\infty^S(\gamma)$ is decreasing for $\gamma \in (0, \gamma_*)$ and increasing for $\gamma \in (\gamma_*, +\infty)$ with $\gamma_* = \xi v_\theta$;

(iv) there exists $M \in \mathbb{N}$ such that $\tilde{\chi}_M^H(\gamma) = \min_{n\in\mathbb{N}} \tilde{\chi}_n^H(\gamma)$ for fixed $\gamma \in (0, +\infty)$.

One can find the proof for Lemma 3.3 in Appendix.B. In a similar way with Lemma 2.4, we can also prove the properties of eigenvalues of Eq.(3.3) as follows.

Lemma 3.4. *Let $\tilde{\chi}_n^S(\gamma)$, $\tilde{\chi}_n^H(\gamma)$, $\tilde{\chi}_\infty^S(\gamma)$ be defined as (3.4), (3.5), (3.7), and $\tilde{\chi}_N^S(\gamma)$, $\tilde{\chi}_M^H(\gamma)$ in Lemma 3.3, we further define*

$$\chi^-(\gamma) = \tilde{\chi}_N^S(\gamma),\ \chi^+(\gamma) = \min\left\{\tilde{\chi}_M^H(\gamma), \tilde{\chi}_\infty^S(\gamma)\right\}. \tag{3.8}$$

Then we have the following results:

(i) *when $\chi^-(\gamma) < \chi < \chi^+(\gamma)$, all the eigenvalues of Eq.(3.3) have negative real parts;*

(ii) *when $\chi \geq \chi^+(\gamma)$, $\mu = \pm i\omega_n$ $(\omega_n > 0)$ is a pair of purely imaginary roots of Eq.(2.7) if $\chi = \tilde{\chi}_n^H(\gamma)$;*

(iii) *when $\chi \leq \chi^-(\gamma)$, $\mu = 0$ is a root of Eq. (2.7) if $\chi = \tilde{\chi}_n^S(\gamma)$.*

Remark 3.5. The boundary curve $\chi = \chi^+(\gamma)$ for the constant steady state of system (1.5) to lose stability consists of two types of bifurcation curve $\chi = \tilde{\chi}_M^H(\gamma)$ or $\chi = \tilde{\chi}_\infty^S(\gamma)$. When the constant steady state loses its stability via $\chi = \tilde{\chi}_\infty^S(\gamma)$, there will be infinitely many eigenvalues with positive real parts for the corresponding linearized system. This situation also happens in an explicit spatial memory model studied in [26].

Similar to Lemma 2.5, we can verify that the following transversality condition for Hopf bifurcation holds in system (1.5) and we omit the proof.

Lemma 3.6. *Let $\chi = \tilde{\chi}_n^H(\gamma)$ be defined as (3.5). Then, Eq.(3.3) has a pair of roots in the form of $\mu = \delta(\chi) \pm i\omega(\chi)$ when χ is near $\tilde{\chi}_n^H(\gamma)$ such that $\delta\left(\tilde{\chi}_n^H(\gamma)\right) = 0$ and $\delta'\left(\tilde{\chi}_n^H(\gamma)\right) > 0$.*

By Lemmas 3.3, 3.4, 3.6 and Hopf bifurcation theory for partial functional differential equations, we obtain the following results on the stability and bifurcation behaviors of the positive homogeneous steady state of Eq.(1.5).

Theorem 3.7. *Assume that condition (A) holds, and let $\tilde{\chi}_n^S(\gamma)$, $\tilde{\chi}_n^H(\gamma)$ be defined as (3.4), (3.5), and $\chi^-(\gamma)$, $\chi^+(\gamma)$ in (3.8), we have the following results for Eq.(1.5):*

(i) a mode-n Turing bifurcation occurs at $\chi = \tilde{\chi}_n^S(\gamma)$ for $\gamma > 0$ and $n \in \mathbb{N}$, thus a mode-n spatially nonhomogeneous steady state can arise near $(\theta, v_\theta, \tilde{q}_\theta)$;

(ii) a mode-n Hopf bifurcation occurs at $\chi = \tilde{\chi}_n^H(\gamma)$ for $\gamma > 0$ and $n \in \mathbb{N}$, and the bifurcating periodic solutions are spatially nonhomogeneous;

(iii) if we fix $\gamma \in (0, +\infty)$, the positive homogeneous steady state $(\theta, v_\theta, \tilde{q}_\theta)$ is locally asymptotically stable for $\chi^-(\gamma) < \chi < \chi^+(\gamma)$ and unstable for $\chi \in (-\infty, \chi^-(\gamma)) \cup (\chi^+(\gamma), +\infty)$.

Taking the parameters as $d_1 = 0.01,\ d_2 = 0.02,\ m = 0.5,\ d = 0.1,\ k = 1,\ b = 0.2,\ \xi = 0.3$, the bifurcation diagram of Eq.(1.5) is illustrated in Fig.5. We see that

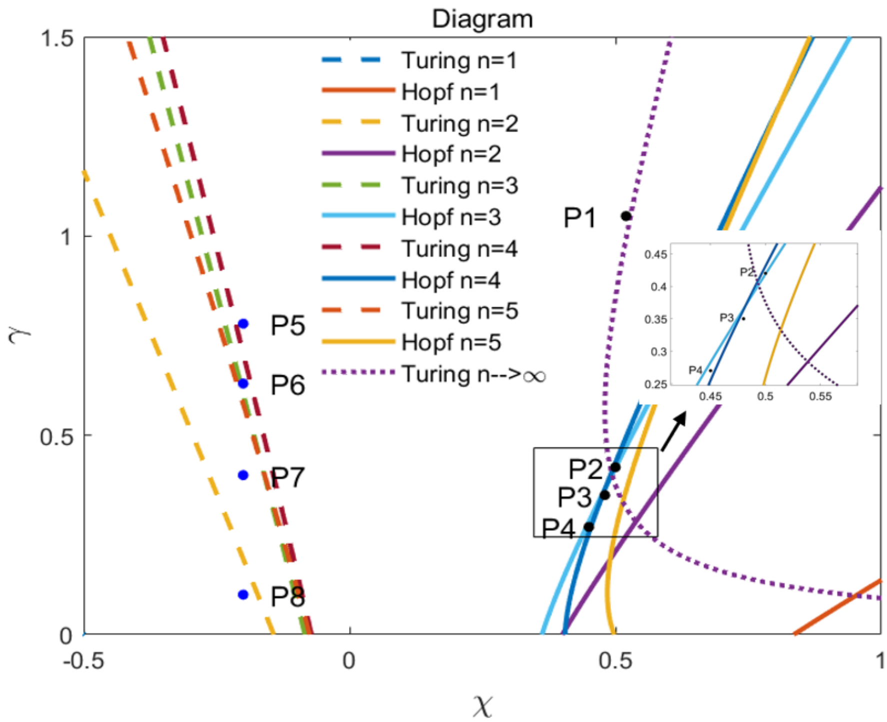

Fig. 5: The bifurcation diagram of system (1.5) in parameter plane (χ, γ) with $d_1 = 0.01$, $d_2 = 0.02$, $m = 0.5$, $d = 0.1$, $k = 1$, $b = 0.2$, $\xi = 0.3$, $\Omega = (0, \pi)$, and the Turing bifurcation curves $\chi = \chi_n^S(\gamma)$ can be identified by the dotted curves and Hopf bifurcation curves $\chi = \chi_n^H(\gamma)$ by the solid curves. The points are parameter values for the numerical simulations and they are: P1 $(0.52, 1.05)$, P2 $(0.50, 0.42)$, P3 $(0.48, 0.35)$, P4 $(0.45, 0.27)$, P5 $(-0.2, 0.78)$, P6 $(-0.2, 0.63)$, P7 $(-0.2, 0.40)$ and P8 $(-0.2, 0.10)$.

the dynamics of (1.5) is different from that of (1.4): i) there exists a limiting Turing curve $\chi = \chi_\infty$ corresponding to the infinite mode which destabilizes the system when $\chi > \chi_\infty$; ii) different modes of Hopf bifurcation curves can intersect with each other such that codimension-2 double Hopf bifurcation occurs. Near the intersection point of mode-3 and mode-4 Hopf bifurcation curves, we choose proper parameter values as presented in P2, P3, and P4 to perform simulations. When the parameters are taken as $(\chi, \gamma) = P2 = (0.50, 0.42)$ which is extremely close to the mode-4 Hopf bifurcation curve, we observe that a mode-4 spatially nonhomogeneous periodic pattern arises as shown in Fig.6(b). When $(\chi, \gamma) = P3$ which is in between the area enclosed by the two Hopf bifurcation curves and $(\chi, \gamma) = P4$ which is closest to the mode-3 Hopf bifurcation curve, we observe a quasi-periodic pattern and a mode-3 periodic pattern, respectively, as illustrated in Fig.6 (c) and (d). Compared to the periodic patterns observed in system (1.4) (see Fig.2), the spatial distribution of resources is more diverse, and even quasi-periodic distribution is possible due to the impact of the consumption process on cognition and memory in system (1.5).

In Fig.7, we illustrate the spatially nonhomogeneous steady state and some wan-

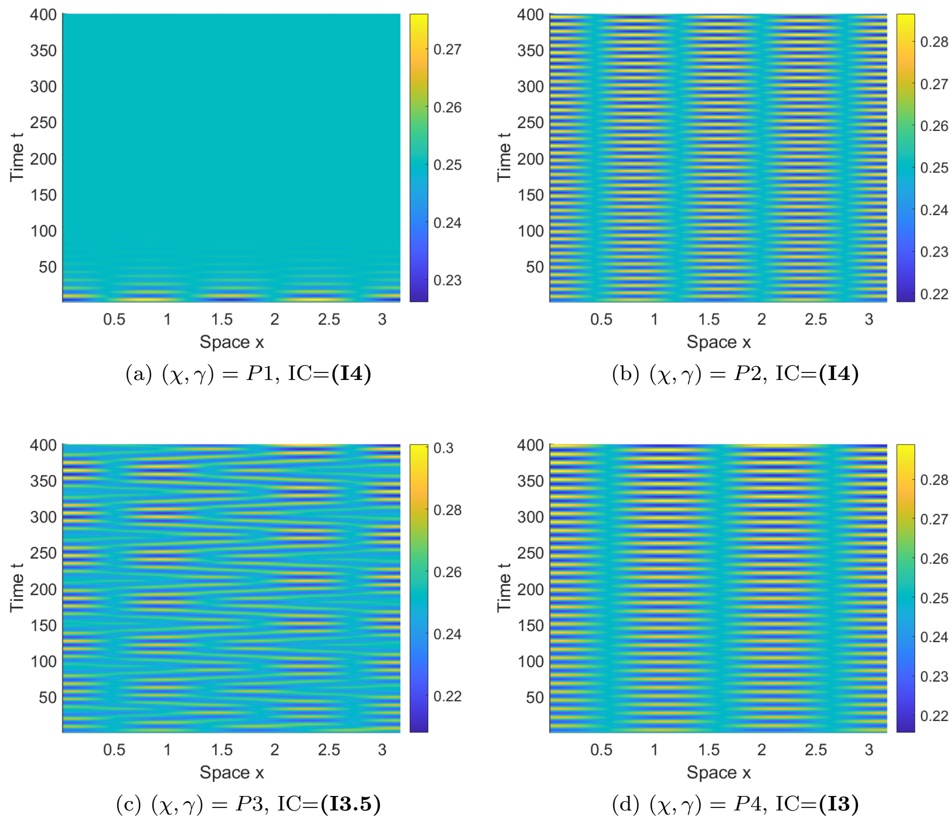

(a) $(\chi, \gamma) = P1$, IC=**(I4)**

(b) $(\chi, \gamma) = P2$, IC=**(I4)**

(c) $(\chi, \gamma) = P3$, IC=**(I3.5)**

(d) $(\chi, \gamma) = P4$, IC=**(I3)**

Fig. 6: Periodic patterns rising near Hopf bifurcation curves in system (1.5) when parameters are $d_1 = 0.01,\ d_2 = 0.02,\ m = 0.5,\ d = 0.1,\ k = 1,\ b = 0.2,\ \xi = 0.3$ and $\Omega = (0, \pi)$. In each figure, the color indicates the value of $u(x, t)$ according to the color bar.

dering periodic patterns when $\chi = -0.2$. When we choose $\gamma = 0.78$ corresponding to P5 in Fig.5, the constant steady state $(\theta, v_\theta, q_\theta)$ is stable as shown in (a). If we decrease γ to 0.63 corresponding to P5 which is under the mode-4 Turing curve, it is shown that a mode-4 spatially nonhomogeneous steady state arises as shown in (b). When we continue to decrease the γ value to 0.40, it can be seen that the mode-4 steady state is still stable as shown in (c). Similar to model (1.4), we observe a "wandering" pattern with a large period for $\gamma = 0.10$ as shown in (d).

4. Discussion. In [35], Wang and Salmaniw summarized three main categories of cognitive processes in animal movement models: perception, memory, and learning. Perception means the ability to see, hear, or otherwise become aware of something through the senses, while memory is the stability to store, retain, and retrieve information [6,10]. Learning is the information acquisition from an individual experience [10]. Spatial memory modeled by explicit time delay has received much attention:

(i) discrete delay: [2,12,24–26,29–32,34,36–38,40];

(ii) distributed delay: [14,23,27,33,41];

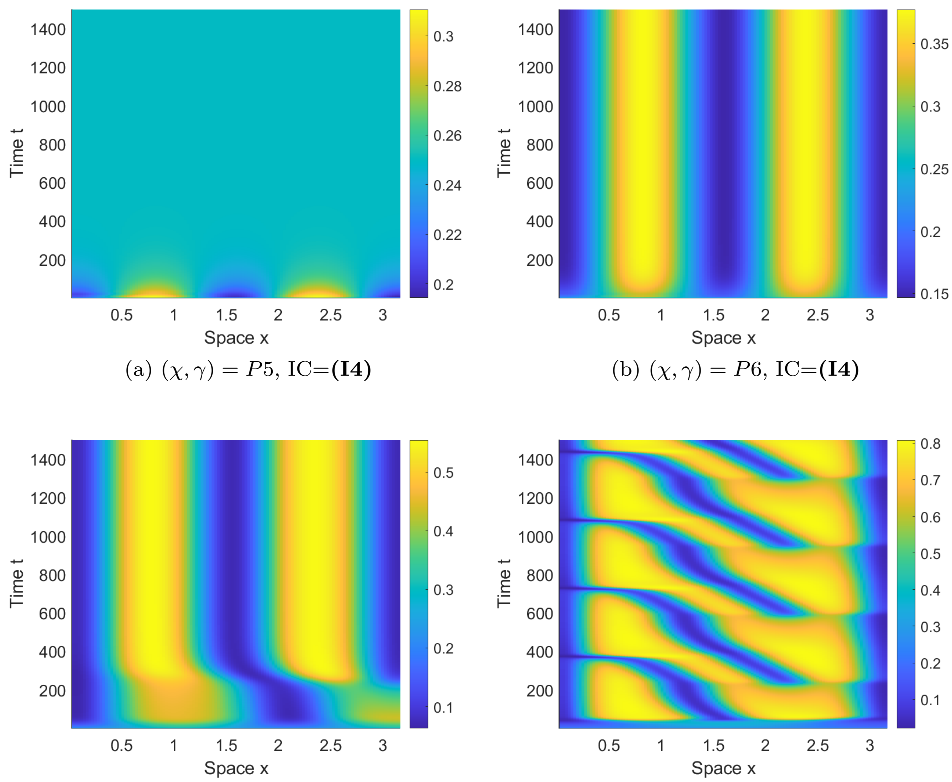

(a) $(\chi, \gamma) = P5$, IC=**(I4)**

(b) $(\chi, \gamma) = P6$, IC=**(I4)**

(c) $(\chi, \gamma) = P7$, IC=**(I3)**

(d) $(\chi, \gamma) = P8$, IC=**(I2)**

Fig. 7: Spatially nonhomogeneous steady state rising near Turing bifurcation curves in system (1.5) when parameters are $d_1 = 0.01,\ d_2 = 0.02,\ m = 0.5,\ d = 0.1,\ k = 1,\ b = 0.2,\ \xi = 0.3$ and $\Omega = (0, \pi)$. In each figure, the color indicates the value of $u(x,t)$ according to the color bar.

(iii) nonlocal delay: [28].

Through these studies, we can gain some insight into the effect of explicit memory in delayed form on animal movement. However, there is little analysis completed for implicit memory that is described by a learning equation [**?**, 35]. In this paper, we consider resource-consumer models with implicit spatial memory by incorporating an additional biased diffusion term which shows an attractive movement of consumers to the resource. The difference between these two models lies in the cognitive potential function $q(x,t)$ satisfying two different learning ODEs. System (1.4)/(1.5) is a PDE-ODE coupled system whose linearized system has a more complicated spectrum than a classical reaction-diffusion system. We first performed a spectral analysis for each system and found that the spectral set of the corresponding linear system for (1.4)/(1.5) is discrete, which implies that the stability of the constant steady state is still determined by the corresponding eigenvalue problem. Next, we took the memory-based diffusion rate $\chi \in \mathbb{R}$ as a bifurcation parameter and performed a bifurcation analysis for system (1.4)/(1.5).

In systems (1.4) and (1.5), steady-state bifurcation and Hopf bifurcation can both occur. From the bifurcation diagram in Figs. 1 and 5, we observe that the constant steady states are stable for a small memory-based diffusion rate (either attractive or repulsive), while a large memory-based diffusion can destabilize the systems and induce rich spatial patterns. The outcome differences between these two models mainly lie in the following two aspects.

1. All the steady-state bifurcation curves lie in the left half plane in $\chi-\gamma$ plane in system (1.4). In system (1.5), there exists an n_* defined in Lemma 3.3 such that the steady-state bifurcation curves move to the right half plane when $n \geq n_*$. In particular, when $n \to +\infty$, we found a limiting Turing curve $\chi = \tilde{\chi}^S_\infty$ such that the linearized system at the constant steady state has infinitely many eigenvalues with positive real parts for $\chi > \tilde{\chi}^S_\infty$.
2. In system (1.4), the dominant mode for Hopf bifurcation will not vary with different memory-based diffusion rates when the other parameters are fixed. For example, we observed that the mode-2 Hopf bifurcation is stable when the parameter values are taken as in Fig. 1. However, it is shown that there are different dominant modes for different memory-based diffusion rates in system (1.5), even two different modes of Hopf bifurcation curve can intersect with each other such that a codimension-2 double Hopf bifurcation occurs, see Figs.5&6.

Based on the above theoretical reasons, the dynamics of system (1.5) are richer, for instance, different modes of stable periodic patterns and quasi-periodic patterns can be found in system (1.5). From a biological perspective, these results indicate that the distribution of the resource/consumer seems more spatially diverse when the cognitive map $q(x,t)$ follows the more realistic learning equation (H2).

This paper considered local perception when the cognitive kernel $g(x)$ is a delta function which is the limiting case when the perceptive range is extremely narrow. However, the actual situation is that the animal has a restricted habitat and wide perceptive range, therefore it is more realistic when the kernel function is taken as a top-hat, Gaussian, or exponential form.

Appendix A: The proof of Theorem 3.1. For $\mu \in \mathbb{C}$ and $(\tau_1, \tau_2, \tau_3) \in Y$, we consider the nonhomogeneous problem

$$\begin{cases} d_1\Delta\phi + \beta\phi - d\psi = \mu\phi + \tau_1, \\ d_2\Delta\psi - \chi v_\theta \Delta\varphi + \alpha\phi = \mu\psi + \tau_2, \\ bv_\theta\phi + \dfrac{b\theta\gamma}{\gamma + \xi v_\theta}\psi - \gamma\varphi = \mu\varphi + \tau_3, \\ \partial_n\phi = \partial_n\psi = 0. \end{cases} \tag{4.1}$$

Case 1: $\mu \neq -\gamma - \xi v_\theta$. From the third equation of (4.1), we can obtain $\varphi = bv_\theta\phi + \dfrac{b\theta\gamma}{\gamma+\xi v_\theta}\psi - \tau_3$ and substitute it into the second equation, we have

$$\begin{cases} d_1\Delta\phi + \beta\phi - d\psi = \mu\phi + \tau_1, \\ d_2\Delta\psi - \dfrac{\chi v_\theta}{\mu+\gamma+\xi v_\theta}\Delta\left(bv_\theta\phi + \dfrac{b\theta\gamma}{\gamma+\xi v_\theta}\psi - \tau_3\right) + \alpha\phi = \mu\psi + \tau_2, \\ \partial_n\phi = \partial_n\psi = 0, \end{cases} \tag{4.2}$$

which is equivalent to

$$\tilde{\mathcal{L}}_1\begin{pmatrix}\phi\\ \psi\end{pmatrix}\begin{pmatrix} d_1\Delta\phi+\beta\phi-d\psi-\mu\phi\\ d_2\Delta\psi-\dfrac{b\chi v_\theta}{\mu+\gamma+\xi v_\theta}\Delta\phi+\alpha\phi-\mu\psi\end{pmatrix}=\begin{pmatrix}\tau_1\\ \tau_2-\dfrac{\chi v_\theta}{\mu+\gamma}\Delta\tau_3\end{pmatrix}.$$

By a similar argument as in the proof of Theorem 2.1, we know that $\tilde{\mathcal{L}}_1$ has a bounded inverse $\tilde{\mathcal{L}}_1^{-1}$ with

$$\begin{aligned}&\|\phi\|_{W^{2,p}(\Omega)}+\|\psi\|_{W^{2,p}(\Omega)}\\ \le&\|\tilde{\mathcal{L}}_1^{-1}\|\left(\|d_1\Delta\phi+\beta\phi-d\psi\|_{L^p(\Omega)}+\left\|d_2\Delta\psi-\frac{b\chi v_\theta}{\mu+\gamma+\xi v_\theta}\Delta\phi+\alpha\phi\right\|_{L^p(\Omega)}\right),\end{aligned}$$

when $\mu\in\mathbb{C}$ satisfies the following inequality

$$(\mu+d_1\lambda_n-\beta)(\mu+\gamma+\xi v_\theta)[(\mu+d_2\lambda_n)(\gamma+\xi v_\theta)-\xi v_\theta b\theta\gamma]+d\alpha(\mu+\gamma+\xi v_\theta)+db\chi v_\theta^2\lambda_n\neq 0. \tag{4.3}$$

Therefore, we know that $\tilde{\mathcal{L}}-(\mu+\xi v_\theta)I$ has a bounded inverse $\left(\tilde{\mathcal{L}}-(\mu+\xi v_\theta)I\right)^{-1}$.

If (4.3) does not hold, then it can be inferred that μ satisfies the dispersal relation (3.3) which has three roots $\tilde{\mu}_n^{(j)}$, $j=1,2,3$ for each $n\in\mathbb{N}_0$. For $j=1,2,3$, we put $\mu=\tilde{\mu}_n^{(j)}$ into (4.1), one can check that $\tilde{\mu}_n^{(j)}$ are indeed eigenvalues of $\tilde{\mathcal{L}}$ with eigenfunctions being

$$\begin{pmatrix}\tilde{\phi}_n^{(j)}\\ \tilde{\psi}_n^{(j)}\\ \tilde{\varphi}_n^{(j)}\end{pmatrix}=\begin{pmatrix}1\\ \dfrac{1}{d}\left(-d_1\lambda_n+\beta-\tilde{\mu}_n^{(j)}\right)\\ \dfrac{dbv_\theta(\gamma+\xi v_\theta)-b\theta\gamma\left(d_1\lambda_n+\tilde{\mu}_n^{(j)}-\beta\right)}{\left(\tilde{\mu}_n^{(j)}+\gamma+\xi v_\theta\right)(\gamma+\xi v_\theta)}\end{pmatrix}\phi_n,$$

which implies that $Ker(\tilde{\mathcal{L}}-\tilde{\mu}_n^{(j)})=Span\left\{\left(\tilde{\phi}_n^{(j)},\tilde{\psi}_n^{(j)},\tilde{\varphi}_n^{(j)}\right)^T\right\}$.

Case 2: $\mu=-\gamma-\xi v_\theta$. Then Eq. (4.1) becomes

$$\begin{cases}d_1\Delta\phi+\beta\phi-d\psi=(\gamma+\xi v_\theta)\phi+\tau_1,\\ d_2\Delta\psi-\chi v_\theta\Delta\varphi+\alpha\phi=(\gamma+\xi v_\theta)\psi+\tau_2,\\ bv_\theta\phi+\dfrac{b\theta\gamma}{\gamma+\xi v_\theta}\psi=\tau_3,\\ \partial_n\phi=\partial_n\psi=0,\end{cases}$$

which can be solved as

$$\begin{cases}d_1\Delta\phi+\left(\beta-\gamma-\xi v_\theta+\dfrac{bdv_\theta(\gamma+\xi v_\theta)}{b\theta\gamma}\right)\phi=\tau_1+\dfrac{d(\gamma+\xi v_\theta)\tau_3}{b\theta\gamma},\\ \psi=\dfrac{(\gamma+\xi v_\theta)(\tau_3-bv_\theta\phi)}{b\theta\gamma},\\ \Delta\varphi=\dfrac{1}{\chi v_\theta}\left(d_2\Delta\psi+\alpha\phi-(\gamma+\xi v_\theta)\psi-\tau_2\right).\end{cases}$$

By letting $\tau_1=\tau_2=\tau_3=0$, we know that the first equation only has trivial solution $\phi=0$ when $\beta-\gamma-\xi v_\theta+\dfrac{bdv_\theta(\gamma+\xi v_\theta)}{b\theta\gamma}\notin\{\lambda_n\}_{n=1}^\infty$. Also, we have

$\psi = 0$ from the second equation and φ is an arbitrary constant, which implies that $Ker\left(\tilde{\mathcal{L}} + (\gamma + \xi v_\theta I\right) = \text{Span}\{(0,0,1)^T\}$ and thus $-\gamma - \xi v_\theta \in \sigma_p(\tilde{\mathcal{L}})$. If $\beta - \gamma - \xi v_\theta + \dfrac{bdv_\theta(\gamma+\xi v_\theta)}{b\theta\gamma} = \lambda_n$ holds for some $n \in \mathbb{N}$, then we have

$$\begin{aligned}\phi &= \tilde{\phi}_n = d_1\phi_n,\ \psi = \tilde{\psi}_n = -\frac{d_1 v_\theta(\gamma+\xi v_\theta)\phi_n}{\theta\gamma},\\ \varphi &= \tilde{\varphi}_n = \frac{1}{\chi\theta v_\theta \gamma} d_1 d_2 v_\theta(\gamma + \xi v_\theta \lambda_n + \alpha d_1 \theta\gamma + d_1 v_\theta(\gamma+\xi v_\theta)^2)\phi_n.\end{aligned}$$

Then we have $-\gamma - \xi v_\theta \in \sigma_p(\tilde{\mathcal{L}})$ with $Ker\left(\tilde{\mathcal{L}} + (\gamma + \xi v_\theta I\right) = \text{Span}\left\{\left(\tilde{\phi}_n, \tilde{\psi}_n, \tilde{\varphi}_n\right)^T\right\}$. To conclude, we have

$$\sigma(\tilde{\mathcal{L}}) = \sigma_p(\tilde{\mathcal{L}}) = \tilde{S} \cup \{-\gamma - \xi v_\theta\}$$

with $\tilde{S}$ defined as (3.2). This completes the proof.

Appendix B: The proof of Lemma 3.3. By the definition of $\tilde{\chi}_n^S(\gamma)$ given in (3.4), we see that $\tilde{\chi}_n^S(\gamma) = Q_n(\gamma)/P_n(\gamma)$ with $Q_n(\gamma)$ and $P_n(\gamma)$ defined as in (3.6). It can be verified that $Q_n(\gamma) > 0$ for all $\gamma > 0$, therefore, the sign of $\tilde{\chi}_n^S(\gamma)$ is determined by the sign of $P_n(\gamma)$. By letting $P_n(\gamma) > 0$, we have

$$\lambda_n < \frac{dv_\theta(\gamma+\xi v_\theta)}{d_1\gamma\theta} \in \left(\frac{dv_\theta}{d_1\theta}, +\infty\right), \tag{4.4}$$

which implies that $P_n(\gamma) > 0$ holds for all $\gamma > 0$ when $\lambda_n < \dfrac{dv_\theta}{d_1\theta}$, and $n_* \in \mathbb{N}$ is the largest integer such that $\lambda_{n_*} < \dfrac{dv_\theta}{d_1\theta}$. When $n \le n_*$, $\tilde{\chi}_n^S(\gamma) < 0$ holds for al $\gamma > 0$. when $n > n_*$, we have

$$P_n(0) = bdv_\theta^2\lambda_n > 0,\ \lim_{\gamma\to+\infty} P_n(\gamma) = -(d_1\lambda_n - \beta)b\theta v_\theta\lambda_n < 0,$$

and

$$\frac{d[P_n(\gamma)]}{d\gamma} = -\frac{(d_1\lambda_n - \beta)b\theta\xi\lambda_n v_\theta^2}{(\gamma+\xi v_\theta)^2} < 0,$$

thus there exists $\gamma_n^* > 0$ such that $P_n(\gamma_n^*) = 0$, and $P_n(\gamma) > 0$ for $\gamma \in (0, \gamma_n^*)$ and $P_n(\gamma) < 0$ for $\gamma \in (\gamma_n^*, +\infty)$. By the fact the $Q_n(\gamma) > 0$, we obtain the results in (i).

As for (ii), we need to know the monotonicity of $\tilde{\chi}_n^S(\gamma)$ with respect to n, thus we first rewrite $\tilde{\chi}_n^S(\gamma)$ as the following form by letting $p = \lambda_n$:

$$\tilde{\chi}_p^S(\gamma) = -\frac{(\gamma+\xi v_\theta)(d_2 p(d_1 p - \beta) + d\alpha)}{bdv_\theta^2 p - (d_1 p - \beta)\frac{b\theta\gamma v_\theta p}{\gamma + \xi v_\theta}}.$$

Taking derivative with respect to p, we have

$$\frac{d[\tilde{\chi}_p^S(\gamma)]}{dp} = -\frac{\gamma+\xi v_\theta}{P_n^2(\gamma)}\left[d_1 d_2 bdv_\theta^2 p^2 + \frac{2d\alpha d_1 b\theta\gamma v_\theta}{(\gamma+\xi v_\theta)}p - \frac{d\alpha(bdv_\theta^2(\gamma+\xi v_\theta) + \beta b\theta\gamma v_\theta)}{(\gamma+\xi v_\theta)}\right].$$

From the expression of $\frac{d[\tilde{\chi}_p^S(\gamma)]}{dp}$, we see that $\frac{d[\tilde{\chi}_p^S(\gamma)]}{dp}$ is a quadratic function of p with positive coefficients for quadratic and linear terms. However, the constant term is negative as $bdv_\theta^2(\gamma+\xi v_\theta)+\beta b\theta\gamma v_\theta>0$ when $\tilde{\chi}_n^S(\gamma)>0$, which implies that $\frac{d[\tilde{\chi}_p^S(\gamma)]}{dp}$ has a unique zero p^* such that $\frac{d[\tilde{\chi}_p^S(\gamma)]}{dp}>0$ for $p\in(0,p^*)$ and $\frac{d[\tilde{\chi}_p^S(\gamma)]}{dp}<0$ for $p\in(p^*,+\infty)$ and $\tilde{\chi}_p^S(\gamma)$ reaches its maximum at p^*. Let $N\in\mathbb{N}$ be the integer such that λ_n is the closest eigenvalue to p^*, then we have $\tilde{\chi}_N^S(\gamma)=\max_{n\in\mathbb{N}}\tilde{\chi}_n^S(\gamma)$ for a fixed $\gamma>0$.

When $\tilde{\chi}_n^S(\gamma)>0$, the constant term in the expression of $\frac{d[\tilde{\chi}_p^S(\gamma)]}{dp}$ is positive, thus we know that $\frac{d[\tilde{\chi}_p^S(\gamma)]}{dp}<0$ from the discussion in the proof of (ii). Therefore, $\tilde{\chi}_n^S(\gamma)$ is strictly decreasing with respect to n and we have

$$\min_{n>n_*}\tilde{\chi}_n^S(\gamma)=\lim_{n\to+\infty}\tilde{\chi}_n^S(\gamma)=\frac{d_2(\gamma+\xi v_\theta^2)}{b\theta\gamma v_\theta}. \tag{4.5}$$

Define the limiting Turing curve as $\tilde{\chi}_\infty^S$ in (3.7), and it can be known that $\tilde{\chi}_\infty^S(\gamma)$ is first decreasing and then increasing function of γ and reaches its minimum at $\gamma=\gamma_*$. This proves the conclusions in (iii).

To prove (iv), we rewrite $\tilde{\chi}_n^H(\gamma)$ as

$$\begin{aligned}\tilde{\chi}_p^H(\gamma)=&\frac{((d_1+d_2)p-\beta)}{bdv_\theta^2p+b\theta\gamma v_\theta p+\frac{d_2b\theta\gamma v_\theta p^2}{\gamma+\xi v_\theta}}\left[d_2p(d_1p-\beta)\right.\\&\left.+(\gamma+\xi v_\theta)((d_1+d_2)p-\beta)+(\gamma+\xi v_\theta)^2+d\alpha\right].\end{aligned}$$

where λ_n in $\tilde{\chi}_n^H(\gamma)$ is replaced by p. Taking the derivative with respect to p, we obtain

$$\frac{d[\tilde{\chi}_p^H(\gamma)]}{dp}=\frac{F_p(\gamma)}{H_p^2(\gamma)},$$

where

$$\begin{aligned}F_p(\gamma)=&H_p(\gamma)\left\{(d_1+d_2)\left[d_2p(d_1p-\beta)+(\gamma+\xi v_\theta)((d_1+d_2)p-\beta)+(\gamma+\xi v_\theta)^2\right.\right.\\&\left.\left.+d\alpha\right]+((d_1+d_2)p-\beta)(2d_1d_2p-\beta+(d_1+d_2)(\gamma+\xi v_\theta))\right\}\\&-Q_p(\gamma)\left(bdv_\theta^2+b\theta\gamma v_\theta+\frac{2d_2b\theta\gamma v_\theta p}{\gamma+\xi v_\theta}\right),\end{aligned}$$

and

$$\begin{aligned}Q_p(\gamma)=&((d_1+d_2)p-\beta)\left[d_2p(d_1p-\beta)+(\gamma+\xi v_\theta)((d_1+d_2)p-\beta)\right.\\&\left.+(\gamma+\xi v_\theta)^2+d\alpha\right],\\H_p(\gamma)=&bdv_\theta^2p+b\theta\gamma v_\theta p+\frac{d_2b\theta\gamma v_\theta p^2}{\gamma+\xi v_\theta}.\end{aligned}$$

By a tedious calculation, one can verify that $F_p(\gamma)$ is a quartic polynomial of p, that is,

$$F_p(\gamma)=a_4(\gamma)p^4+a_3(\gamma)p^3+a_2(\gamma)p^2+a_1(\gamma)p+a_0(\gamma)$$

with

$$
\begin{aligned}
a_4(\gamma) &= \frac{(d_1+d_2)d_1d_2^2 b\theta\gamma v_\theta}{\gamma+\xi v_\theta} > 0,\\
a_0(\gamma) &= \beta(bdv_\theta^2 + b\theta\gamma v_\theta)[\alpha + (\gamma+\xi v_\theta)^2 - \beta(\gamma+\xi v_\theta)] < 0.
\end{aligned}
$$

Therefore, it can be inferred that there exists at least one positive zero $p = p^{**}$ of $F_p(\gamma)$ such that $\tilde{\chi}_p^H(\gamma)$ reaches its minimum at $p = p^{**}$. Therefore, we may take $M \in \mathbb{N}$ such that λ_M is the closest eigenvalue to p^{**}. This completes the proof.

Acknowledgements. The first author is partially supported by the National Natural Science Foundation of China (No.12001240,12271216) and the Natural Science Foundation of Jiangsu Province (No.BK20200589). The second author is supported by the National Natural Science Foundation of China (No.12371166) and the Zhejiang Provincial Natural Science Foundation of China (No.LZ23A010001). The third author is partially supported by the Natural Sciences and Engineering Research Council of Canada (Individual Discovery Grant RGPIN-2020-03911 and Discovery Accelerator Supplement Award RGPAS-2020-00090) and the Canada Research Chairs program (Tier 1 Canada Research Chair Award).

REFERENCES

[1] B. Abrahms, E. L. Hazen, E. O. Aikens, M. S. Savoca, J. A. Goldbogen, S. J. Bograd, M. G. Jacox, L. M. Irvine, D. M. Palacios, and B. R. Mate, *Memory and resource tracking drive blue whale migrations*, Proc. Natl. Acad. Sci., 116 (2019), pp. 5582–5587.

[2] Q. An, C. C. Wang, and H. Wang, *Analysis of a spatial memory model with nonlocal maturation delay and hostile boundary condition*, Discrete Contin. Dyn. Syst., 40 (2020), pp. 5845–5868, https://doi.org/10.3934/dcds.2020249.

[3] S. S. Chen, J. P. Shi, and G. H. Zhang, *Spatial pattern formation in activator-inhibitor models with nonlocal dispersal*, Discrete Contin. Dyn. Syst. Ser. B, 26 (2021), pp. 1843–1866, https://doi.org/10.3934/dcdsb.2020042, https://doi.org/10.3934/dcdsb.2020042.

[4] W. F. Fagan, *Migrating whales depend on memory to exploit reliable resources*, Proc. Natl. Acad. Sci., 116 (2019), pp. 5217–5219.

[5] W. F. Fagan, E. Gurarie, S. Bewick, A. Howard, R. S. Cantrell, and C. Cosner, *Perceptual ranges, information gathering, and foraging success in dynamic landscapes*, Am. Nat., 189 (2017), pp. 474–489.

[6] W. F. Fagan, M. A. Lewis, M. Auger-Méthé, T. Avgar, S. Benhamou, G. Breed, L. LaDage, U. E. Schlägel, W. W. Tang, Y. P. Papastamatiou, J. Forester, and T. Mueller, *Spatial memory and animal movement*, Ecology Letters, 16 (2013), pp. 1316–1329.

[7] A. P. Foss-Grant, *Quantitative challenges in ecology: competition, migration, and social learning*, PhD thesis, University of Maryland, 2017.

[8] R. Golledge, *Wayfinding Behavior: Cognitive Mapping and Other Spatial Processes*, Johns Hopkins University Press, 1998.

[9] D. Henry, *Geometric Theory of Semilinear Parabolic Equations [electronic resource]*, Springer, New York, 1981.

[10] M. A. Lewis, W. F. Fagan, M. Auger-Méthé, J. Frair, J. M. Fryxell, C. Gros, E. Gurarie, S. D. Healy, and J. A. Merkle, *Learning and animal movement*, Front. Ecol. Evol., 9 (2021), p. 681704.

[11] M. A. Lewis and J. D. Murray, *Modelling territoriality and wolf–deer interactions*, Nature, 366 (1993), pp. 738–740.

[12] S. Li, S. L. Yuan, Z. Jin, and H. Wang, *Bifurcation analysis in a diffusive predator-prey model with spatial memory of prey, Allee effect and maturation delay of predator*, J. Differ. Equ., 357 (2023), pp. 32–63, https://doi.org/10.1016/j.jde.2023.02.009.

[13] Y. Li, A. Marciniak-Czochra, I. Takagi, and B. Y. Wu, *Bifurcation analysis of a diffusion-ode model with turing instability and hysteresis*, Hiroshima Math. J., 47 (2017), pp. 217–247, https://doi.org/10.32917/hmj/1499392826.

[14] J. Lin and Y. L. Song, *Spatially inhomogeneous periodic patterns induced by distributed memory in the memory-based single population model*, Appl. Math. Lett., 137 (2023), p. 108490, https://doi.org/10.1016/j.aml.2022.108490.

[15] A. Marciniak-Czochra, G. Karch, and K. Suzuki, *Instability of turing patterns in reaction-diffusion-ode systems*, J. Math. Biol., 74 (2017), pp. 583–618, https://doi.org/10.1007/s00285-016-1035-z.

[16] P. R. Moorcroft and M. A. Lewis, *Mechanistic home range analysis*, Princeton University Press, 2006.

[17] P. R. Moorcroft, M. A. Lewis, and R. L. Crabtree, *Home range analysis using a mechanistic home range model*, Ecology, 80 (1999), pp. 1656–1665.

[18] J. O'Keefe and L. Nadel, *The Hippocampus as a Cognitive Map*, Oxford University Press, 1978.

[19] K. J. Painter and T. Hillen, *Spatio-temporal chaos in a chemotaxis model*, Phys. D, 240 (2011), pp. 363–375.

[20] J. R. Potts and M. A. Lewis, *How memory of direct animal interactions can lead to territorial pattern formation*, J. R. Soc. Interface, 13 (2016), p. 20160059.

[21] J. R. Potts and M. A. Lewis, *Spatial memory and taxis-driven pattern formation in model ecosystems*, Bull. Math. Biol., 81 (2019), pp. 2725–2747.

[22] U. E. Schlägel and M. A. Lewis, *Detecting effects of spatial memory and dynamic information on animal movement decisions*, Methods Ecol. Evol., 5 (2014), pp. 1236–1246.

[23] H. Shen, Y. L. Song, and H. Wang, *Bifurcations in a diffusive resource-consumer model with distributed memory*, J. Differ. Equ., 347 (2023), pp. 170–211, https://doi.org/10.1016/j.jde.2022.11.044.

[24] J. P. Shi, C. C. Wang, and H. Wang, *Diffusive spatial movement with memory and maturation delays*, Nonlinearity, 32 (2019), pp. 3188–3208.

[25] J. P. Shi, C. C. Wang, and H. Wang, *Spatial movement with diffusion and memory-based self-diffusion and cross-diffusion*, J. Differ. Equ., 305 (2021), pp. 242–269, https://doi.org/10.1016/j.jde.2021.10.021.

[26] J. P. Shi, C. C. Wang, H. Wang, and X. P. Yan, *Diffusive spatial movement with memory*, J. Dyn. Differ. Equ., 32 (2020), pp. 979–1002.

[27] Q. Y. Shi, J. P. Shi, and H. Wang, *Spatial movement with distributed memory*, J. Math. Biol., 82 (2021), p. 33, https://doi.org/10.1007/s00285-021-01588-0.

[28] Q. Y. Shi and Y. L. Song, *Spatial movement with nonlocal memory*, Discrete Contin. Dyn. Syst. Ser. B, 28 (2023), pp. 5580–5596, https://doi.org/10.3934/dcdsb.2023067.

[29] Y. L. Song, Y. H. Peng, and T. H. Zhang, *The spatially inhomogeneous Hopf bifurcation induced by memory delay in a memory-based diffusion system*, J. Differ. Equ., 300 (2021), pp. 597–624, https://doi.org/10.1016/j.jde.2021.08.010.

[30] Y. L. Song, Y. H. Peng, and T. H. Zhang, *Double hopf bifurcation analysis in the memory-based diffusion system*, J. Dyn. Diff. Equat., (2022), https://doi.org/10.1007/s10884-022-10180-z.

[31] Y. L. Song, J. P. Shi, and H. Wang, *Spatiotemporal dynamics of a diffusive consumer-resource model with explicit spatial memory*, Stud. Appl. Math., 148 (2022), pp. 373–395, https://doi.org/10.1111/sapm.12443.

[32] Y. L. Song, S. H. Wu, and H. Wang, *Spatiotemporal dynamics in the single population model with memory-based diffusion and nonlocal effect*, J. Differ. Equ., 267 (2019), pp. 6316–6351, https://doi.org/10.1016/j.jde.2019.06.025.

[33] Y. L. Song, S. H. Wu, and H. Wang, *Memory-based movement with spatiotemporal distributed delays in diffusion and reaction*, Appl. Math. Comput., 404 (2021), p. 126254, https://doi.org/10.1016/j.amc.2021.126254.

[34] C. H. Wang, S. L. Yuan, and H. Wang, *Spatiotemporal patterns of a diffusive prey-predator model with spatial memory and pregnancy period in an intimidatory environment*, J. Math. Biol., 84 (2022), p. 12, https://doi.org/10.1007/s00285-022-01716-4.

[35] H. Wang and Y. Salmaniw, *Open problems in PDE models for knowledge-based animal movement via nonlocal perception and cognitive mapping*, J. Math. Biol., 86 (2023), p. 71, https://doi.org/10.1007/s00285-023-01905-9.

[36] Y. J. Wang, D. J. Fan, and C. C. Wang, *Dynamics of a single population model with memory effect and spatial heterogeneity*, J. Dyn. Diff. Equat., 34 (2022), pp. 1433–1452, https://doi.org/10.1007/s10884-021-10010-8.

[37] Y. J. Wang, D. J. Fan, C. C. Wang, and Y. M. Chen, *Dynamics of a predator-prey model with memory-based diffusion*, J. Dyn. Diff. Equat., (2023). https://doi.org/10.1007/s10884-023-10305-y.

[38] Y. J. Wang, C. C. Wang, and D. J. Fan, *Dynamics of a diffusive competition model with*

memory effect and spatial heterogeneity, J. Math. Anal. Appl., 523 (2023), p. 126991, https://doi.org/10.1016/j.jmaa.2022.126991.

[39] S. Y. Xue, Y. L. Song, and H. Wang, *Spatio-temporal dynamics in a reaction-diffusion equation with non-local spatial memory*, SIAM J. Appl. Dyn. Syst., 23 (2024), pp. 641–667.

[40] H. Zhang, H. Wang, Y. L. Song, and J. J. Wei, *Diffusive spatial movement with memory in an advective environment*, Nonlinearity, 36 (2023), pp. 4585–4614.

[41] H. Zhang, H. Wang, and J. J. Wei, *Perceptive movement of susceptible individuals with memory*, J. Math. Biol., 86 (2023), p. 65, https://doi.org/10.1007/s00285-023-01904-w.